NMR study of localized electrons in conductive Langmuir-Blodgett films

Hiroshi Tsukada
Graduate School of Human and Environmental Studies, Kyoto University, Yoshida Nihonmatsu-cho, Sakyo-ku, Kyoto 606-8316, Japan
(Received 10 April 1998; revised manuscript received 31 July 1998)

An investigation of nuclear spin lattice relaxation was performed on a conductive Langmuir-Blodgett (LB) film based on a charge-transfer (CT) complex of bisethylenedioxytetrathiafulvalene (BO) and decyltetracyanoquinodimethane (C_{10}TCNQ). The characteristic peak of the relaxation rate T_1^{-1} of ^{1}H was observed at a low temperature (10 K). As in its pristine solid (BO-C_{10}TCNQ complex), the behavior of the relaxation rate was explained by the theory of localization. From the quantitative analysis of the behavior, the detailed dynamics of the localized electrons in the LB film were successfully obtained. In addition, the outer-planar anisotropy of T_1^{-1} of ^{1}H was observed in the LB film. This indicates that the observed echo mainly originated from ^{1}H at the end ethylene groups of BO. The fact that the field dependence of this anisotropic T_1^{-1} is well fitted by the cosine curve provides detailed information of the hyperfine structures in the LB film. Considering these results in combination with those of the temperature dependence of T_1^{-1}, it is concluded that the variance of each level of BO is small and that the nature of disorder in the LB film is that of a continuum. [S0163-1829(99)05703-3]

I. INTRODUCTION

Langmuir-Blodgett (LB) films based on the donor molecule of bisethylenedioxytetrathiafulvalene (BO) have recently been the subject of much interest because of their flexible design ability of two-dimensional (2D) molecular assembly and their stability in ultrathin metallic systems.[1–3]

A conductive LB film formed from a charge-transfer (CT) complex of BO and decyltetracyanoquinodimethane (C_{10}TCNQ) and from icosanoic acid achieved the macroscopically metallic nature without doping for the first time.[1] The temperature dependence of the conductivity of the BO-C_{10}TCNQ LB film is at its maximum at around 250 K. Below this temperature, the conductivity shows an exponential decrease due to a percolation effect.[4] Thus the nature of this film reflects the existence of the semiconducting domain boundaries.

A recent paper has reported that LB film formed from BO and behenic acid preserves metallic conductivity down to a considerably low temperature (14 K).[3] The stability of the metallic state of this film originates from the realization of the uniform layered structure of BO. This stability also indicates that the effect of the domain boundaries is strongly suppressed. The semiconducting domain boundaries thus play an important part in this wide difference of macroscopic electrical conductivity.

Atomic force microscopy measurement of the BO-C_{10}TCNQ LB film has shown that the film structure is granular with a domain size of 1 μm.[5] Electron spin resonance (ESR) measurement has demonstrated that the spin susceptibility of the BO-C_{10}TCNQ LB film is separated following two temperature domains: (1) Pauli susceptibility which originates from conduction electrons in BO above 50 K; (2) Curie-like susceptibility below 50 K.[6] The former behavior indicates the existence of 2D metallic domains composed of BO stacks.

The former behavior is consistent with the linear temperature dependence of thermoelectric power.[1] It should be noted that the origin of the Curie component may be attributed to disorders.[6] Therefore, we expect that localized electrons exist in the LB film. In our previous paper, we reported that the nuclear relaxation rate of ^{1}H in BO-C_{10}TCNQ powder exhibited a peak at low temperatures.[7] We proposed that the peak can be interpreted as Anderson localization in weakly disordered systems. We therefore considered that the detection of the localization in the LB film can also be made by the NMR method.

Especially at low temperatures, Anderson localization, which is the interference effect of electron waves, becomes a matter of great importance rather than the ''particle'' image of electrons in the form of the propagation of electron wave packets. The reason for this is that the inelastic scatterings fall off along with the decrease in temperature. In order to obtain highly stable metallic LB films, we must explore this localization mechanism that hinders the stability.

Accordingly, we here investigate, to our knowledge for the first time, the localized electrons and the nature of disorders in conductive LB film by measuring the spin lattice relaxation time of ^{1}H in the BO-C_{10}TCNQ LB film, particularly in the low-temperature region of 2–14 K.

II. EXPERIMENT

The BO-C_{10}TCNQ complex is prepared by mixing two hot solutions of each component. The composition is $(BO)_{10}(C_{10}TCNQ)_4(H_2O)$ from the elemental analysis.[8] In the preparation of the LB sample, the horizontal lifting method was adopted. The sample consisted of 200 monolayers that correspond to about 2 mg in the weight of BO. A silicon sheet with a thickness of 1 mm was used as substrate. The acetonitrile solution of the BO-C_{10}TCNQ complex with a molar concentration of 5×10^{-4} mol/l in the unit of C_{10}TCNQ and the benzene solution of icosanoic acid with a concentration of 5×10^{-4} mol/l were mixed at the same volume ratio. The temperature dependence of the ^{1}H nuclear spin lattice relaxation time T_1 was measured at the resonance

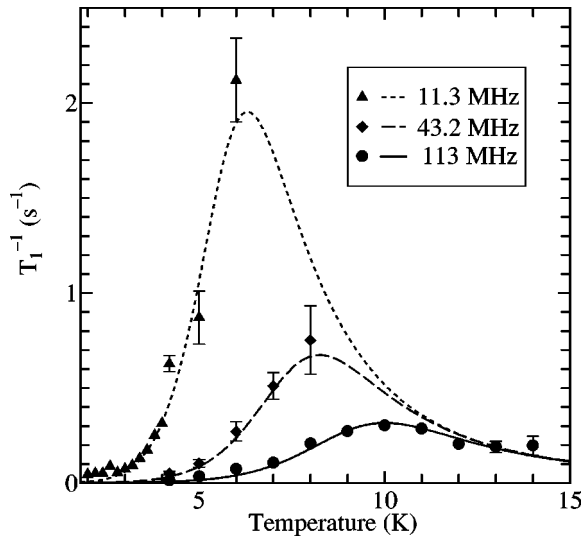

FIG. 1. The temperature dependence of T_1^{-1} of ^{1}H in the BO-C_{10}TCNQ LB film at 11.3, 43.2 and 113 MHz. The solid curve is fitted by the theoretical formula [Eq. (1)] for localization in weakly disordered systems. The broken curves are reproductive, using the parameters in Table I. The behaviors of the increase at 11.3 and 43.2 NHz are consistent with the frequency dependence of Eq. (1) as a whole.

frequency of 11.3 and 43.2 MHz in the temperature range of 2–8 K, using single- and three-coil geometry, respectively. The direction of the external field was normal to the substrate. Despite the high accumulation of the LB film (200 layers), the observed spin echo collapsed into the thermally activated noises above 5 K at 11.3 MHz and above 8 K at 43.2 MHz. To protect the echo from the fluctuation of the noises, the resonance frequency was sharply increased up to 113 MHz. In addition, the frequency of the integration was also increased. This suppressed the effect of the noises and allowed the measurement up to a higher temperature (14 K). The outer-planar anisotropy of the ^{1}H nuclear spin lattice relaxation time was measured at 4.2 K and the resonance frequency of 43.2 MHz.

III. RESULTS AND DISCUSSIONS

A. Dynamics of the localized electrons in the LB film

Figure 1 represents the plots of the relaxation rate versus temperature at the frequencies of 11.3, 43.2, and 113 MHz. As the temperature becomes higher, the relaxation rate at 11.3 MHz increases gradually, and then makes a drastic increase at above 3 K. Similarly, the rate at 43.2 MHz exhibits a characteristic increase over 4.2 K, but the increase is more gradual than that at 11.3 MHz.

At both frequencies, the errors of the data plots are increasingly enhanced with the increase of the temperature. This indicates that the errors can be ascribed to the thermally activated noises.

For this reason, the measurement of the temperature dependence of the T_1 was also carried out at still higher frequency (113 MHz). In consequence, the higher field prevented the data plots from fluctuating and the peak of the relaxation rate was successfully observed at 10 K. But the enhancement of the rate itself was still more suppressed than in the case of the rate at 43.2 MHz.

TABLE I. The fitted parameters in Eq. (1).

ω_e	A	B	C	p
113 MHz	6.67×10^{9}	6.04×10^{6}	8.49×10^{-4}	5

With regard to the drastic increase and the peak of T_1^{-1} of the LB film, the following three possible causes can be proposed: (1) antiferromagnetic spin ordering, (2) molecular motions, and (3) disorders.

The first possibility is eliminated by the temperature dependence of the ESR linewidth of the film. With regard to the second possibility, the Bloembergen-Purcell-Pound peak due to the motion of the end ethylene groups of the well-known donor bisethylenedithiotetrathiafulvalene (BEDT-TTF) has been observed over 250 K.[9,10] But taking into account the temperature region of the nuclear magnetic resonance (NMR) measurement, it is difficult to explain the increase and the peak by the second possibility. As will be discussed later, these two possibilities are completely ruled out by the observation of anisotropic T_1. As to the last possibility, we have already mentioned in Sec. I that the relaxation rate of the BO-C_{10}TCNQ powder exhibits the peak due to Anderson localization at low temperatures.[7]

The solid curve in Fig. 1 is a fitted curve of the data at 113 MHz by the theory of localization in weakly disordered systems. If the lifetime of electrons in the localized state $\tau_{\rm in}$ follows power-law dependence $\tau_{\rm in}=kT^p$, the theoretical curve is expressed as[7]

$$T_1^{-1}=C\left[T+\frac{BT^{p+1}}{T^{2p}+A}\right],\quad A=\left(\frac{\omega_e}{k}\right)^2,\quad B=\frac{1}{2\tau_c k},\quad (1)$$

where C is the Korringa constant, ω_e the resonance frequency, and τ_c the localization time.

The fitted parameters are listed in Table I.

The broken curves in Fig. 1 are reproduced by using these parameters. As shown in Fig. 1, these curves closely follow the behaviors of the increase of the rate at 11.3 and 43.2 MHz.

From Eq. (1) and the values in Table I, we obtain values of k and τ_c as $k=8.75\times10^{3}\ {\rm s^{-1}\,K^{-5}}$, $\tau_c^{-1}=1.06\times10^{11}\ {\rm s^{-1}}$.

The hopping transition temperature $T_{\rm c}$ is determined by the formula of $\tau_{\rm in}(T_{\rm c})=\tau_c$. Therefore, we can estimate the temperature as $T_{\rm c}=\sqrt[5]{1/k\tau_c}=2.61\times10$ K.

The exponent $p=5$ of $\tau_{\rm in}$ in the BO-C_{10}TCNQ LB film is larger than that of the BO-C_{10}TCNQ powder ($p=3$). Furthermore, the $T_{\rm c}$ of the BO-C_{10}TCNQ LB film (=26.1 K) is higher than that of the BO-C_{10}TCNQ powder (=18.9 K). These results suggest that the dimensionality of phonons and the electronic mean free path for elastic scattering are different between the LB film and its pristine solid.

B. Anisotropy of the relaxation rate in the LB film

In the BO-C_{10}TCNQ LB film, the anisotropy is observed with respect to the g value and the linewidth for conduction electron spins in BO, while those for TCNQ spins exhibit no

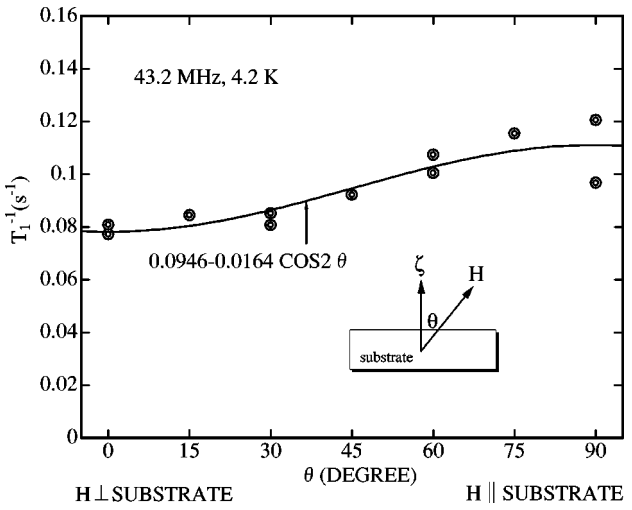

FIG. 2. The outer-planar anisotropy of T_1^{-1} of ^{1}H in the BO-C_{10}TCNQ LB film at 43.2 MHz and 4.2 K.

clear anisotropy.[11] The anisotropy is a clear evidence of the ''orientational'' order of BO molecules in the LB film.

As shown in Fig. 2, the relaxation rate in the LB film at 4.2 K exhibits clear anisotropy according to the outer-planar direction of the external field. The anisotropy of T_1 is caused by the anisotropic hyperfine coupling due to the dipole interaction between the electron spin and nuclear spin of ^{1}H of BO. These facts clearly indicate that the observed echo consists mostly of the hyperfine field at the protons of BO.

Below, we will discuss the details of this anisotropic hyperfine structure and evaluate it quantitatively.

C. Hyperfine field tensor of protons at the end ethylene groups of BO

The hyperfine field of protons at the end ethylene groups of BO consists mostly of the following two components: (1) the isotropic core term at the proton site in question and (2) the anisotropic dipole term from the electron spin at the adjacent carbon site. As shown in Fig. 3(a), we introduce the axes of the end ethylene group. We set up the y axis normal to the plane of H-C-H union. Then the hyperfine field tensor **A** of protons at the end ethylene group of BO is given by

$$\mathbf{A}=\sigma_{\mathrm{H}}\begin{bmatrix}\alpha & 0 & 0\\ 0 & \alpha & 0\\ 0 & 0 & \alpha\end{bmatrix}+\sigma_c\begin{bmatrix}-\beta_c & 0 & 0\\ 0 & -\beta_c & 0\\ 0 & 0 & 2\beta_c\end{bmatrix}, \quad (2)$$

where $\alpha=(8\pi/3)\mu_{\mathrm{B}}|\psi(0)|^2$ is the core-polarization term. Taking into consideration the core term at the proton site, the wave function of 1s orbital ψ_{1s} can reasonably be taken as ψ.

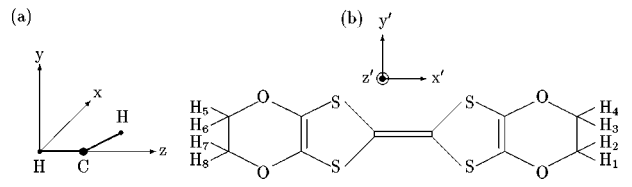

FIG. 3. (a) The definition of axes of the end ethylene group. (b) The definition of the molecular axes of BO.

Then the core term α is reduced to $8\mu_{\mathrm{B}}/3r_0^3=1.78\times10^2$ kOe, where r_0 is the Bohr radius ($=0.529$ Å). $\beta_c=\mu_{\mathrm{B}}/r_{\mathrm{H\text{-}C}}^3$ is the dipole term, which is estimated to be 1.68×10 kOe, using C-H bond length ($=0.95$ Å). σ_c and σ_{H} are the spin densities at the carbon and the proton site of the end ethylene group, respectively.

We replace $\sigma_{\mathrm{H}}\alpha$ and $\sigma_c\beta_c$ with a and b, respectively. Then the expression for $(T_1T)^{-1}$ in terms of a_q, b_q is expressed by[12]

$$\frac{1}{T_1T}=\frac{\gamma_I^2k_{\mathrm{B}}}{2(\gamma_e\hbar)^2}\sum_q\frac{\chi_q''(\omega)}{\omega}[(7-3\cos2\theta)b_qb_{-q}+4a_qa_{-q}-(1+3\cos2\theta)(a_qb_{-q}+a_{-q}b_q)], \quad (3)$$

where θ is the angle between the symmetry axis (z axis) and the direction of external field, and q is the scattering vector.

D. Analysis of anisotropic T_1^{-1} in the LB film

As shown in the Appendix, we see that the macroscopic hyperfine field tensor $\mathbf{A}^{\mathrm{sub}}$ is equivalent to **A** except for the slight correction of the dipole term. So, we replace b with κb in Eq. (3). If we consider only the uniform part, the frequency dependence of $\chi''_{q=0}(\omega)$ is linear. Therefore, the frequency parts of Eq. (3) cancel each other and the dynamical susceptibility χ'' is turned into a static one. We then obtain the following expression for the outer-planar anisotropy of the relaxation rate:

$$\left(\frac{1}{T_1T}\right)_\theta^{\mathrm{LB}}=\Gamma\left[\left(a^2-\frac{\kappa}{2}ab\right)-\frac{3}{2}\kappa ab\cos2\theta\right], \quad (4)$$

where θ is the angle between the symmetric axis (ζ axis) and the direction of the external field. (The small term κ^2b^2 is neglected; $\Gamma=4.4\times10^{-3}$.) We used the experimental value of spin susceptibility of the BO-C_{10}TCNQ LB film: $\chi_{\mathrm{spin}}^{\mathrm{LB}}=1.2\times10^{-4}$(emu/mol).[6]

Figure 2 represents the outer-planar anisotropy of the relaxation rate. At 43.2 MHz and 4.2 K, the rate varies according to

$$T_1^{-1}=0.0946-0.0164\cos2\theta. \quad (5)$$

Equation (5) includes the additional term due to localization.[13] This term corresponds to the second term in the right side of Eq. (1). By subtracting the term, we obtain the following result for the outer-planar anisotropy:

$$\left(\frac{1}{T_1T}\right)=1.01\times10^{-3}-1.74\times10^{-4}\cos2\theta. \quad (6)$$

If we put $\theta=0$ in Eq. (6), we obtain $(T_1T)^{-1}=8.36\times10^{-4}\simeq C$. This is consistent with the fitted result of the temperature dependence of T_1^{-1}. Comparing Eq. (6) with Eq. (4), we obtain $a=0.24$ kOe, $b=0.36$ kOe. From the above values, we can estimate σ_{H} and σ_c to be 0.001 and 0.02, respectively. The remarkably small spin densities at the end ethylene group qualitatively correspond to their HOMO calculated by the extended Hückel method.[8]

E. The nature of disorders in the LB film

The localization time τ_c of the LB film ($=9.43\times10^{-12}$ s) is more than 20 times shorter than that of the BO-C_{10}TCNQ powder ($=2.10\times10^{-10}$ s). This indicates that the BO-C_{10}TCNQ LB film has a much larger concentration of disorders.

On the other hand, the absolute value of the relaxation rate of the LB film is much smaller than that of the BO-C_{10}TCNQ powder. This is possibly due to the difference in the strength of the disorders. In the vicinity of the Anderson transition, the existential probability density at the disordered lattice is enhanced due to localization. The degree of the enhancement is determined by the strength of disorder $\delta=W/D$, where W is the width of the distribution of each molecular level and D the tight-binding bandwidth.[14]

First, we must note that a well-defined correlation between the absolute value of T_1^{-1} and the concentration N_c of Curie spins has been confirmed by an ^{1}H NMR study in heavily doped polyacetylene.[15] The absolute value of T_1^{-1} is almost proportional to N_c. This behavior is well explained by the spin diffusion motion through the spatially fixed paramagnetic impurities.[16] The small absolute value of T_1^{-1} in the BO-C_{10}TCNQ LB film suggests that the concentration of the Curie-like nature of BO spins in the LB film is much smaller than that in the powder.

Secondly, taking into account that the origin of Curie spins is ascribed to the localized electrons due to disorders, there is also a good correlation between δ and N_c in terms of the Anderson model. In the Anderson model, as δ increases, the ''tails'' of localized states added to the original tight-binding band become longer. Eventually, the mobility edges of the band move inward and decrease the width of the extended states.[14] Therefore, as δ increases more electrons are localized.

Based on the above discussion, we conclude that, despite the larger concentration of disorders, the variance of the individual levels of BO in the LB film is smaller than that of the levels of BO in the BO-C_{10}TCNQ powder.

IV. CONCLUSIONS

In this study, the nuclear spin lattice relaxation rate of a conductive LB film was measured for the first time. The measurement of the spin lattice relaxation rate for the BO-C_{10}TCNQ LB film has demonstrated that both the system and the BO-C_{10}TCNQ powder are closely related to Anderson localization.

The hopping transition temperature T_c is estimated to be 25.9 K. This weak activation by phonons indicates that there is another mechanism of phonon scatterings.

The clear observation of anisotropy of the relaxation rate indicates that the resultant T_1 originates from the hyperfine field due to conduction electrons of BO. The dependence of outer-planar anisotropy is well fitted by the cosine curve. This indicates that the origin of anisotropy is the hyperfine dipole interaction between the electron spin and ^{1}H nuclear spin of BO. Moreover, the obtained spin density is qualitatively consistent with the calculated HOMO by the extended Hückel method.

The smaller absolute value of T_1^{-1} in the LB film indicates that the distribution width W of each molecular level of BO is narrower than that of the powder. Therefore, the absolute value of the relaxation rate correlates with the concentration of the Curie-like component of BO spins. In addition, the larger concentration of disorder of the LB film indicates that the nature of disorder is different between the powder and the LB film.

Finally, the question remains as to what elements cause the nature of disorders to differ from those in the powder. One possible interpretation is as follows.

In the BO-C_{10}TCNQ powder, the nature of the disorder is topological. The reason for this is that the countercomponent ($=C_{10}$TCNQ) directly influences the BO conductive layers. On the other hand, we must note that the promoter (=icosanoic acid) of the separated layered structure exists in the LB film. Thus, the nature of the disorder in the LB film can be ascribed to a continuum disorder that is weakly affected by the random distribution of the countercomponents ($=C_{10}$TCNQ and icosanoic acid). To clarify this matter, a more detailed investigation of these films will be required.

ACKNOWLEDGMENTS

The author is particularly grateful to Professor T. Ishiguro for allowing the use of a device for LB films and for his constant encouragement. I also thank Dr. K. Ogasawara for experimental advice and assistance in the preparation of the LB sample. I thank Professor T. Goto for offering a phase-coherent NMR spectrometer, and Professor K. Mizoguchi for his comments concerning the nuclear relaxation due to paramagnetic impurities. Finally, I thank Professors G. Saito and H. Yamochi for their many stimulating discussions and helpful consultations and Dr. S. Horiuchi not only for providing the BO-C_{10}TCNQ complex but also for his fruitful comments and enlightening suggestions.

APPENDIX A: EVALUATION OF HYPERFINE STRUCTURE IN THE LB FILM

In contrast to powders, BO conductive layers are formed with some ''orientational'' order in the LB film. The in-plane anisotropy of conductivity is not detected. It follows that the layers are uniformly distributed in the film plane. But taking account of thickness of the LB film, the layers are distributed almost parallel to the film plane. This fact is confirmed by the previous measurement of IR Spectra (Ag mode) of BO in the LB film.[11] For this reason, we expect the anisotropy of the relaxation rate according to the outer-planar direction of the external field.

In order to analyze this anisotropy, we must evaluate the hyperfine field tensor from the macroscopic viewpoint.

A detailed discussion of the hyperfine structure is given in the following appendices.

1. One-molecular hyperfine field tensor of the donor

As shown in Fig. 3(b), we determine the molecular axes of BO, where the z' axis is normal to the molecular plane and the x' axis is in the direction of the center double bond of the donor.

Suppose the Eulerian rotatory transform $\mathbf{R}(\alpha_i,\beta_i,\gamma_i)\mathbf{r}(x,y,z)\Rightarrow\mathbf{r}(x',y',z')$, where α_i,β_i, and γ_i

TABLE II. The Eulerian angles at each proton site.

No. (i)	$\sin^2\beta_i\cos^2\gamma_i$	$\cos^2\beta_i$	$\sin 2\beta_i\cos\gamma_i$
1	0.601 312	0.162 936	−0.626 021
2	0.005 096	0.972 189	0.140 772
3	0.448 798	0.128 199	0.479 731
4	0.041 364	0.869 092	0.379 203
5	0.058 383	0.973 887	0.105 822
6	0.481 137	0.143 205	−0.524 98
7	0.004 529	0.990 669	0.133 965
8	0.598 459	0.084 773	0.450 480

are the Eulerian angles which connect the atomic axes involving the ith proton with the molecular axes of BO.

Then the averaged one-molecular hyperfine field tensor $\mathbf{A}^{\mathrm{mol}}$ with the contribution of eight protons is given by

$$\mathbf{A}^{\mathrm{mol}}=\frac{1}{8}\sum_{i=1}^{8}\mathbf{R}(\alpha_i,\beta_i,\gamma_i)\mathbf{A}\mathbf{R}^{-1}(\alpha_i,\beta_i,\gamma_i). \tag{A1}$$

The primary values A_{11}^{mol}, A_{22}^{mol}, and A_{33}^{mol} are

$$A_{11}^{\mathrm{mol}}=\frac{1}{8}\sum_{i=1}^{8}\sum_{j=1}^{3}(R_{1j}^{(i)})^2A_{jj}=a-\frac{b}{8}\sum_{i=1}^{8}(1-3\cos^2\gamma_i\sin^2\beta_i), \tag{A2}$$

$$A_{22}^{\mathrm{mol}}=\frac{1}{8}\sum_{i=1}^{8}\sum_{j=1}^{3}(R_{2j}^{(i)})^2A_{jj}=a-\frac{b}{8}\sum_{i=1}^{8}(1-3\sin^2\gamma_i\sin^2\beta_i), \tag{A3}$$

$$A_{33}^{\mathrm{mol}}=\frac{1}{8}\sum_{i=1}^{8}\sum_{j=1}^{3}(R_{3j}^{(i)})^2A_{jj}=a-\frac{b}{8}\sum_{i=1}^{8}(1-3\cos^2\beta_i). \tag{A4}$$

The Eulerian angles at each proton site are listed in Table II.

2. Macroscopic hyperfine field tensor in the LB film

The 2D conduction originates from the overlap of the π-electron orbital, which projects perpendicularly out of the molecular plane. Therefore, in pristine solid BO complexes in general, the symmetric axis of the BO conductive layer is about normal to the z' axis.

On the other hand, the situation is different in LB films. As a result of the competition in length between the molecular plane and the alkyl chain of fatty acids, the plane has an inclination to the symmetric axis of substrate. In the BO-C_{10}TCNQ LB film, ESR and IR measurements have made it clear that the inclination between the symmetric axis of the substrate and the x' axis is 32°, and that the y' axis lies in the substrate[11] [Fig. 4(a)].

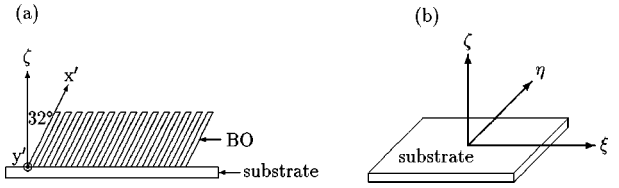

FIG. 4. (a) Schematic relation of the BO molecular plane and substrate. (b) The definition of the outer-planar axes of the substrate.

We replace the angle (=32°) with $(\pi/2)-\beta'$ and determine the outer-planar axes of the substrate as shown in Fig. 4(b).

Then, the hyperfine field tensor $\mathbf{A}^{\mathrm{sub}}$ based on the outer-planar axes is given by

$$\mathbf{A}^{\mathrm{sub}}=\mathbf{R}(0,\beta',\gamma')\mathbf{A}^{\mathrm{mol}}\mathbf{R}^{-1}(0,\beta',\gamma'), \tag{A5}$$

where β',γ' are the Eulerian angles which connect the outer-planar axes with the molecular axes. The molecular axes of x',y' are randomly distributed on the substrate. Therefore, we average $\mathbf{A}^{\mathrm{sub}}$ over γ'. Then Eq. (A5) yields

$$\mathbf{A}^{\mathrm{sub}}=\begin{bmatrix}A_{11}^{\mathrm{sub}} & A_{12}^{\mathrm{sub}} & 0\\ -A_{12}^{\mathrm{sub}} & A_{22}^{\mathrm{sub}} & 0\\ 0 & 0 & A_{33}^{\mathrm{sub}}\end{bmatrix}, \tag{A6}$$

$$A_{11}^{\mathrm{sub}}=A_{22}^{\mathrm{sub}}=\tfrac{1}{2}(A_{11}^{\mathrm{mol}}+A_{22}^{\mathrm{mol}})+\tfrac{1}{2}[\sin^2\beta'(A_{33}^{\mathrm{mol}}-A_{11}^{\mathrm{mol}})-\sin 2\beta' A_{13}^{\mathrm{mol}}], \tag{A7}$$

$$A_{33}^{\mathrm{sub}}=\sin^2\beta' A_{11}^{\mathrm{mol}}+\cos^2\beta' A_{33}^{\mathrm{mol}}+\sin 2\beta' A_{13}^{\mathrm{mol}}, \tag{A8}$$

$$A_{12}^{\mathrm{sub}}=\tfrac{1}{2}\cos\beta'(A_{12}^{\mathrm{mol}}-A_{21}^{\mathrm{mol}})+\tfrac{1}{2}\sin\beta'(A_{23}^{\mathrm{mol}}-A_{32}^{\mathrm{mol}}). \tag{A9}$$

Taking into account the fact that the Eulerian rotatory transform matrix $\mathbf{R}$ is unitary, the off-diagonal elements of $\mathbf{A}^{\mathrm{mol}}$ are symmetric. Thus the off-diagonal elements of $\mathbf{A}^{\mathrm{sub}}$ vanish. Consequently, $\mathbf{A}^{\mathrm{sub}}$ is reduced to the uniaxial symmetric tensor as

$$\mathbf{A}^{\mathrm{sub}}=\begin{bmatrix}a-\kappa b & 0 & 0\\ 0 & a-\kappa b & 0\\ 0 & 0 & a+2\kappa b\end{bmatrix}, \tag{A10}$$

$$\kappa=\tfrac{3}{16}\sum_{i=1}^{8}[\cos^2\beta'\cos^2\beta_i+\sin^2\beta'\sin^2\beta_i\cos^2\gamma_i+\tfrac{1}{2}\sin 2\beta'\sin 2\beta_i\cos\gamma_i]-\tfrac{1}{2}. \tag{A11}$$

From the values listed in Table II, we estimate $\kappa=7.2\times10^{-2}$.

[1] T. Nakamura, G. Yunome, R. Azumi, M. Tanaka, H. Tachibana, M. Matsumoto, S. Horiuchi, H. Yamochi, and G. Saito, J. Phys. Chem. **98**, 1882 (1994).

[2] K. Ogasawara, T. Ishiguro, S. Horiuchi, H. Yamochi, G. Saito, and Y. Nogami, Jpn. J. Appl. Phys., Part 2 **35**, L571 (1996).

[3] H. Ohnuki, T. Noda, M. Izumi, T. Imakubo, and R. Kato, Phys. Rev. B **55**, 10 225 (1997).

[4] K. Ogasawara, T. Ishiguro, S. Horiuchi, H. Yamochi, G. Saito, and Y. Nogami, J. Phys. Chem. Solids **58**, 39 (1996).

[5] T. Nakamura, G. Yunome, R. Azumi, M. Tanaka, M. Yumura, M.

Matsumoto, S. Horiuchi, H. Yamochi, and G. Saito, Synth. Met. **57**, 3853 (1993).

[6] K. Ikegami, S. Kuroda, T. Nakamura, G. Yunome, M. Matsumoto, S. Horiuchi, H. Yamochi, and G. Saito, Phys. Rev. B **49**, 10 806 (1994).

[7] H. Tsukada, T. Goto, K. Ogasawara, S. Horiuchi, H. Yamochi, and G. Saito, J. Phys. Soc. Jpn. **67**, 1556 (1998).

[8] S. Horiuchi, H. Yamochi, G. Saito, K. Sakaguchi, and M. Kusunoki, J. Am. Chem. Soc. **118**, 8604 (1996).

[9] P. Wzietek, H. Mayaffre, D. Jérome, and S. Brazovskii, J. Phys. I **6**, 2011 (1996).

[10] A. V. Skripov, B. A. Aleksashin, Yu. G. Cherepanov, and D. S. Sibirtsev, Phys. Solid State **39**, 32 (1997).

[11] K. Ikegami, S. Kuroda, T. Nakamura, R. Azumi, G. Yunome, M. Matsumoto, S. Horiuchi, H. Yamochi, and G. Saito, Synth. Met. **71**, 1909 (1995).

[12] A. Kawamoto, K. Miyagawa, Y. Nakazawa, and K. Kanoda, Phys. Rev. Lett. **74**, 3455 (1995).

[13] E. P. Nakhmedov, V. N. Prigodin, and Yu. A. Firsov, Zh. Éksp. Teor. Fiz. **92**, 2133 (1987) [Sov. Phys. JETP **65**, 1202 (1987)].

[14] J. M. Ziman: *Models of Disorder*, 1st ed. (Cambridge University Press, Cambridge, 1979), Chap. 9, pp. 359–362.

[15] K. Mizoguchi, Jpn. J. Appl. Phys., Part 1 **34**, 1 (1995).

[16] A. Abragam: *The Principles of Nuclear Magnetism*, 1st ed. (Clarendon, Oxford, 1961), Chap. 9, p. 458.